

Supplemental Figure 1.

(A) Principal component analysis (PCA) of all GIST specimens (top) and only *KIT*, *PDGFRA*, and *SDH*-deficient specimens (bottom) as calculated by DESeq2 for R (n=75, clinicopathologic characteristics are available in Supplemental Table 1).

Supplemental Figure 2.

(A) (top) ESTIMATE and (bottom) Cyt scores by mitotic rate (left) and tumor sizes (middle and right) in all *KIT* and *PDGFRA*-mutant GISTs (n=61). (B) (top) ESTIMATE and (bottom) Cyt scores by mitotic rate (left) and tumor sizes (middle and right) in UPG *KIT* and *PDGFRA*-mutant GISTs (n=22). (C) ESTIMATE scores by mitotic rate in (left) UPG *KIT* and (right) UPG *PDGFRA*-mutant GISTs. High mitotic rate = ≥ 5 mitoses/hpf. Low mitotic rate = < 5 mitoses/hpf. UPG = untreated, primary, gastric. * $p < 0.05$, t-test. Bars, median.

Supplemental Figure 3.

(A) Demonstration of overfitting. On the left, using all 117 immune features to develop the random forest model on the All *KIT* vs. All *PDGFRA* training set (n=50) results in a 72.7% accuracy (red font) on the testing set (n=11). Decreasing the number of features included to 10, 8, and 6 results in an improvement in model accuracy on the testing set to 72.7%, 81.8%, and 90.9% respectively. (B) Retrained All *KIT* vs. All *PDGFRA* model with the top 6 features identified in Figure 6A excluded. (Left) Random forest modeling with 5-fold cross-validation of *KIT* and *PDGFRA*-mutant GIST specimens was performed. Training set created by partitioning 80% (n=50) of *KIT* and *PDGFRA* samples from Supplemental Table 3. Confusion matrix (middle) indicates assessment of model fit to training set. (Left) Predictive capacity of model on remaining *KIT* and *PDGFRA*-mutant GIST testing set (n=11), showing decreased classifier performance to 72.7% (red). Accuracy, sensitivity, specificity, and p-value [Acc > No Information Rate] of models are shown, as calculated by caret package for R.

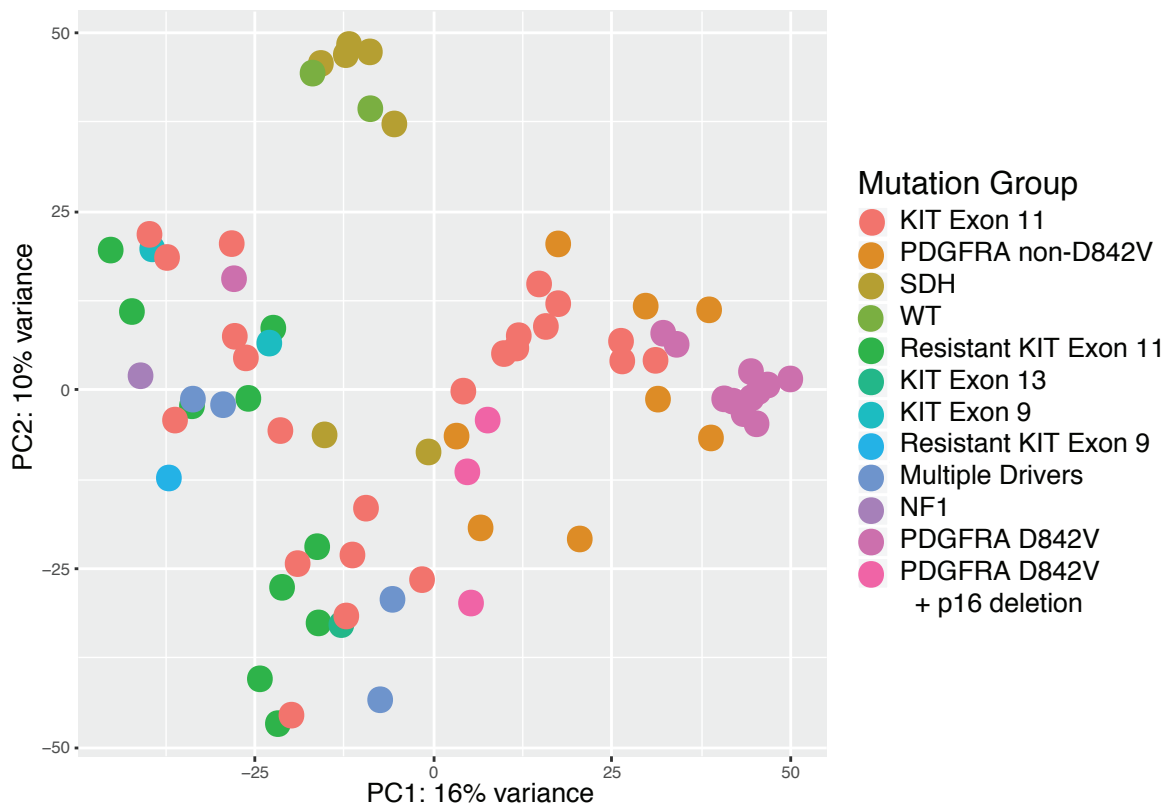
Supplemental Figure 4.

(A) ESTIMATE and Cyt scores in *PDGFRA*-mutant GIST samples that were correctly classified as *PDGFRA*-mutant (n=14) and incorrectly classified as *KIT*-mutant (n=6) by our All *KIT* vs. All *PDGFRA*-mutant random forest model (Figure 6A-C). (B) Distribution of top 6 features identified by random forest modeling in *KIT*-mutant tumors correctly classified as *KIT* and incorrectly classified as *PDGFRA* by our All *KIT* and All *PDGFRA*-mutant random forest model.

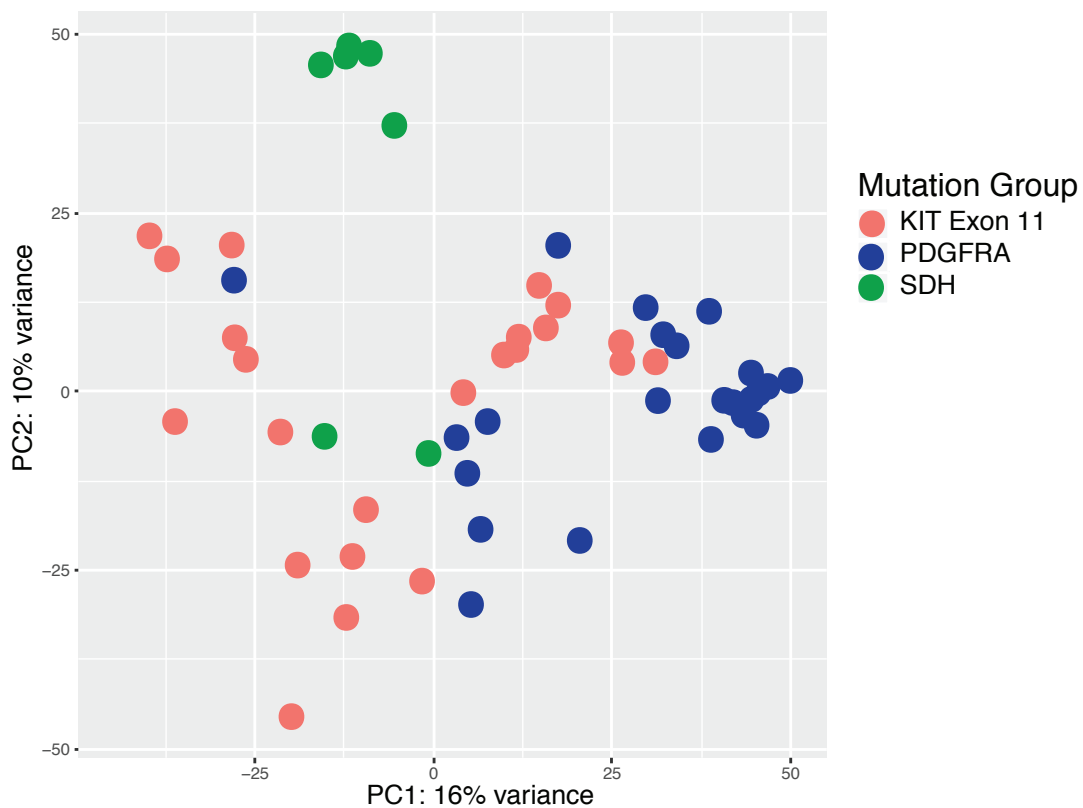
Supplemental Figure 5.

Western blot showing PD-L1 protein expression correlates with PD-L1 mRNA expression calculated by DESeq2. Human GIST numbers and mutation status are shown. KIT = *KIT*-mutant, SDHD = *SDH*-deficient.

Supplemental Figure 1

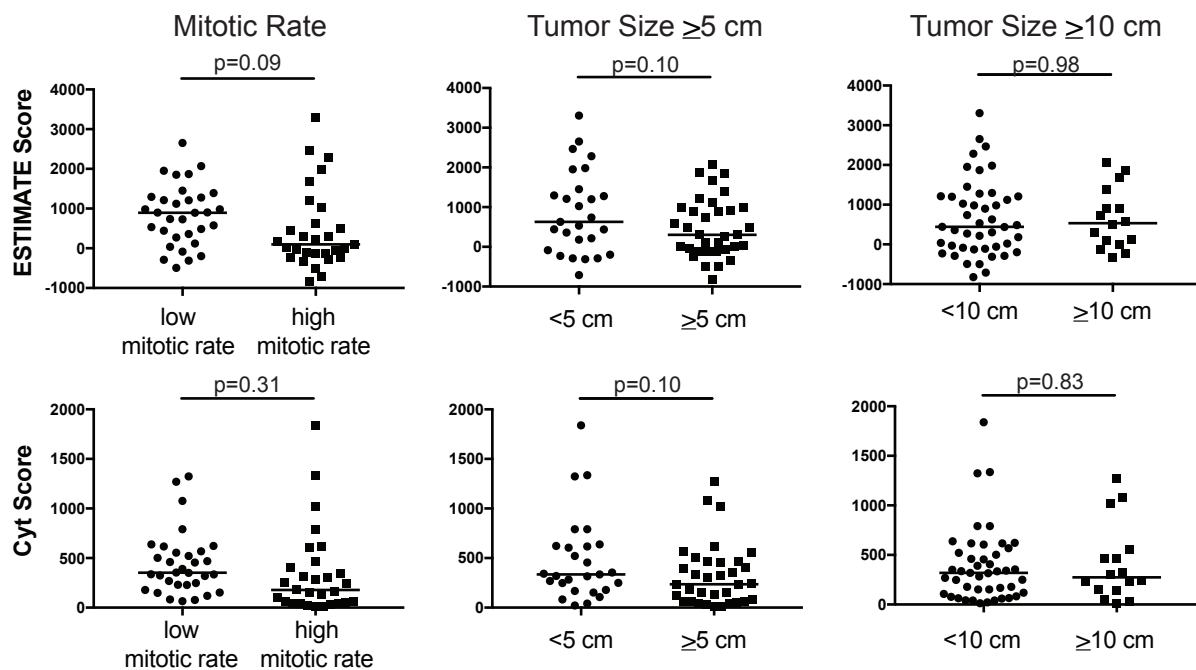


Only KIT, PDGFRA, and SDH shown for clarity

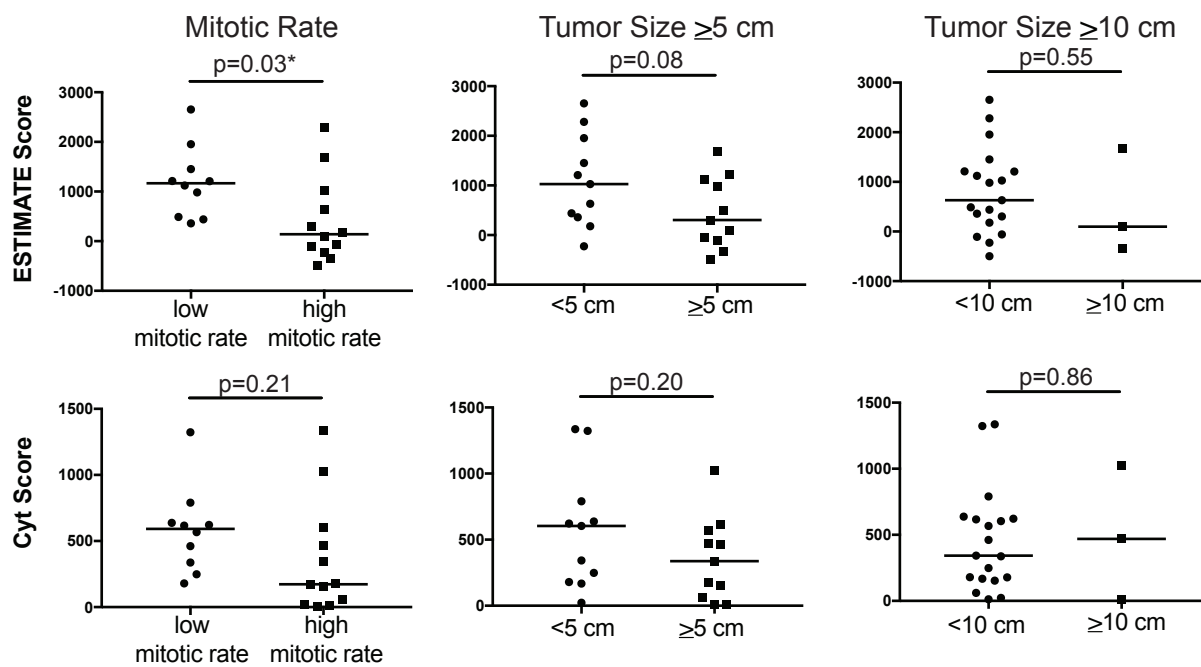


Supplemental Figure 2

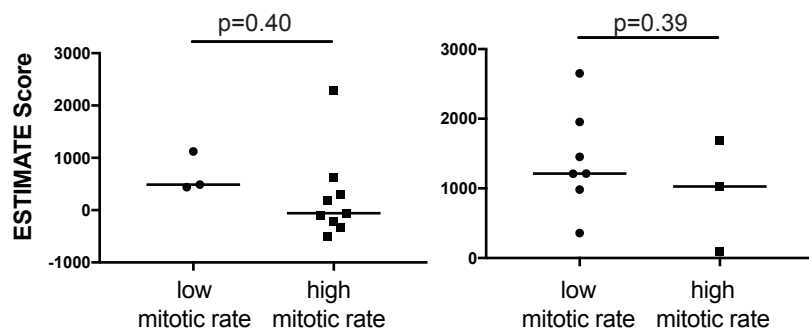
A ALL KIT and PDGFRA-Mutant GISTs (n=61)



B UPG KIT and PDGFRA-Mutant GISTs (n=22)



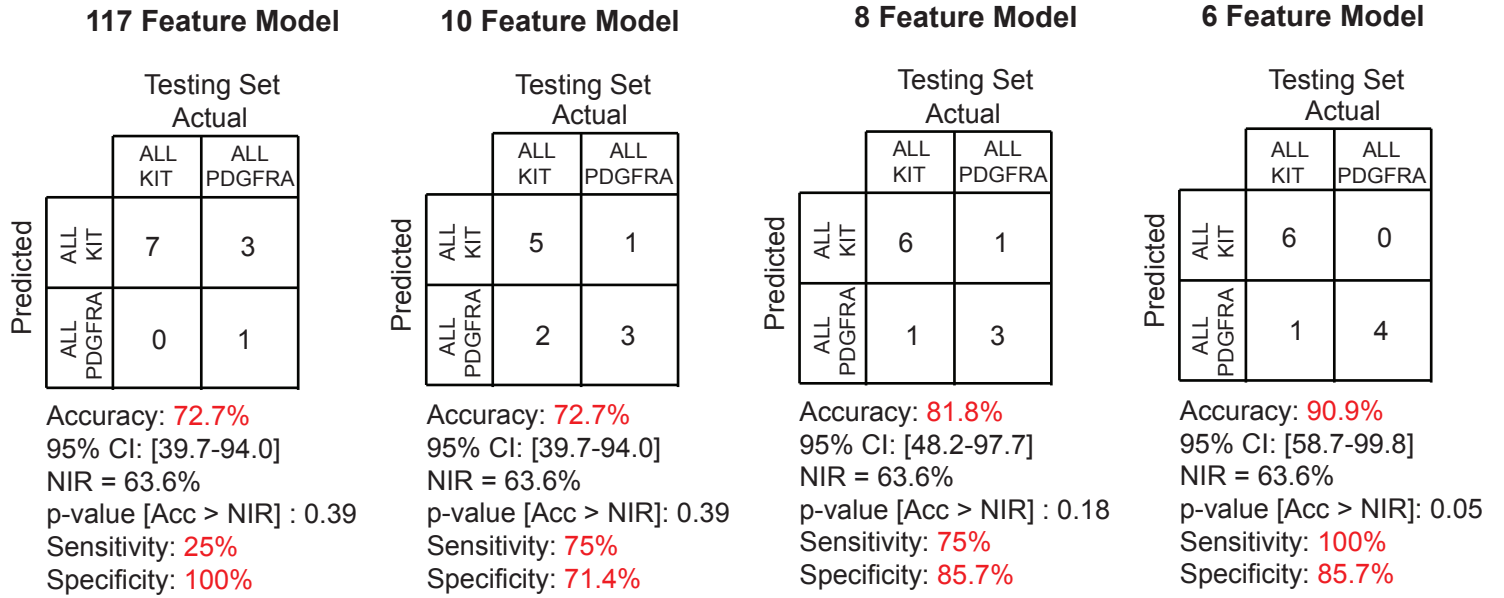
C UPG KIT GISTs UPG PDGFRA GISTs



Supplemental Figure 3

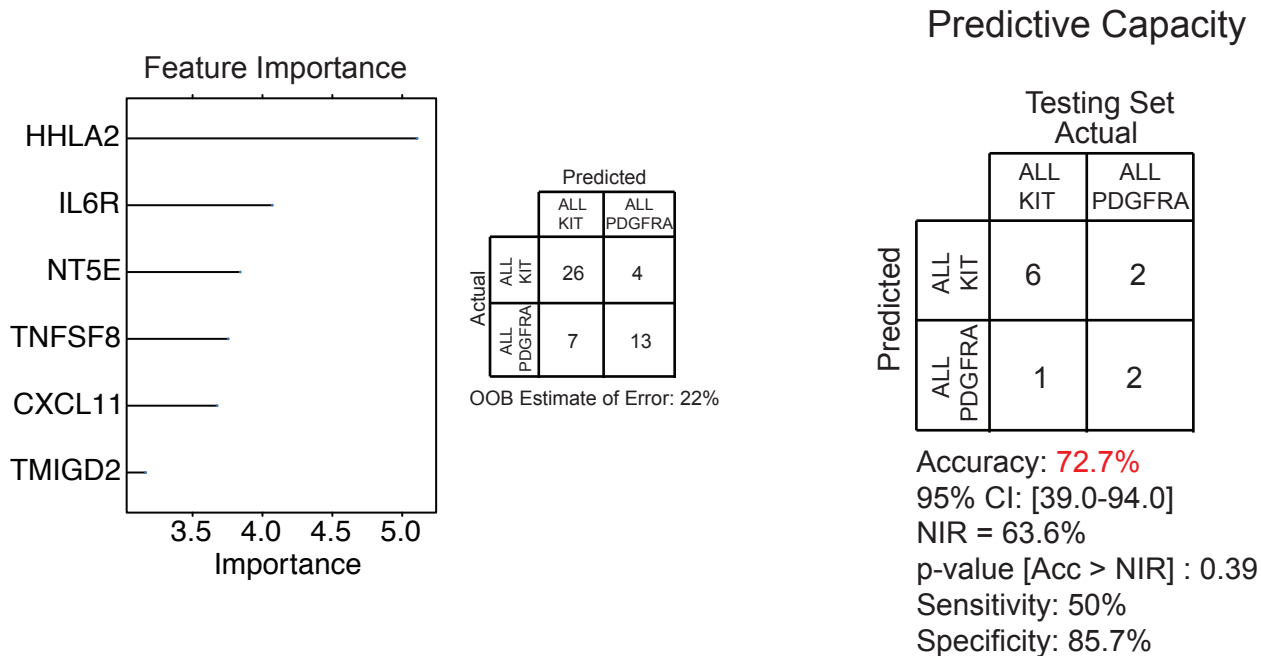
A

Increasing Model Performance with Fewer Model Features (Prevention of Overfitting)

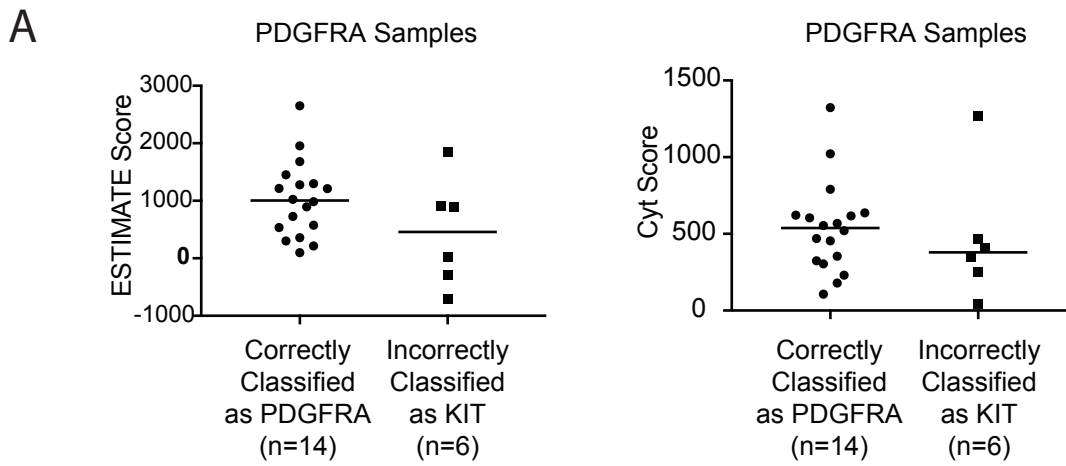


B

Retrained All KIT vs. All PDGFRA Model with Top 6 Features Excluded

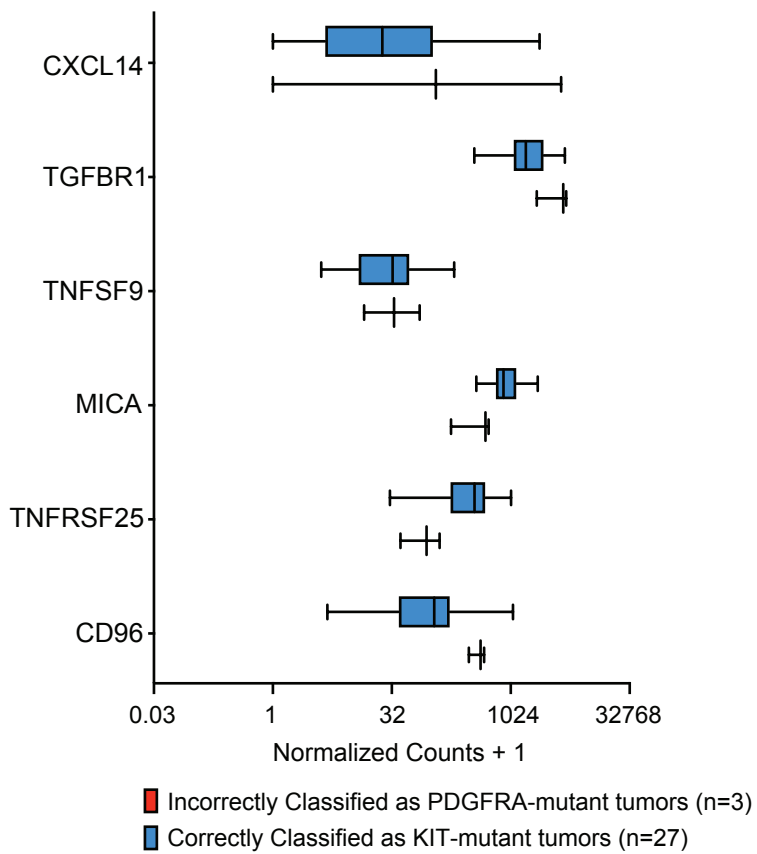


Supplemental Figure 4



B

Distribution of Important Features Among KIT-mutant Tumors



Supplemental Figure 5

Human GIST # 243 218 260 412 257 170 245 295

Mutation KIT KIT KIT SDHD KIT KIT KIT KIT

PD-L1

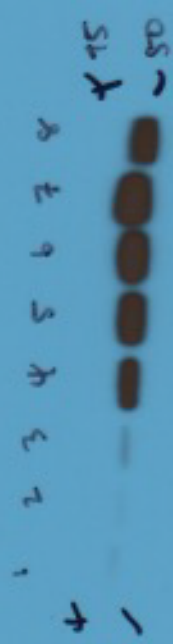


GAPDH



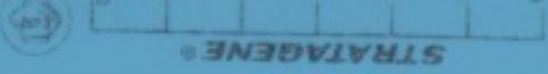
PD-L1 mRNA 34 75 137 267 676 820 839 2500

30-20
D-20



15
50

- | | |
|----------|------|
| 1. H6243 | 34 |
| 2. H6248 | 75 |
| 3. H6260 | 137 |
| 4. H6412 | 267 |
| 5. H6287 | 676 |
| 6. H6190 | 820 |
| 7. H6285 | 839 |
| 8. H6295 | 2510 |



1 sec
pxo

GARDH

